TDP-43 is intercellularly transmitted across axon terminals

Marisa S. Feiler,[1] Benjamin Strobel,[4] Axel Freischmidt,[1] Anika M. Helferich,[1] Julia Kappel,[1] Bryson M. Brewer,[5] Deyu Li,[5] Dietmar R. Thal,[2] Paul Walther,[3] Albert C. Ludolph,[1] Karin M. Danzer,[1]* and Jochen H. Weishaupt[1]*

[1]Department of Neurology, Ulm University, Ulm 89081, Germany
[2]Laboratory for Neuropathology, Institute of Pathology and [3]Central Facility for Electron Microscopy, Ulm University, 89081 Ulm, Germany
[4]Target Discovery Research, Boehringer Ingelheim Pharma GmbH & Co. KG, 88397 Biberach an der Riss, Germany
[5]Department of Mechanical Engineering, Vanderbilt University, Nashville, TN 37212

Transactive response DNA-binding protein 43 kD (TDP-43) is an aggregation-prone prion-like domain-containing protein and component of pathological intracellular aggregates found in most amyotrophic lateral sclerosis (ALS) patients. TDP-43 oligomers have been postulated to be released and subsequently nucleate TDP-43 oligomerization in recipient cells, which might be the molecular correlate of the systematic symptom spreading observed during ALS progression. We developed a novel protein complementation assay allowing quantification of TDP-43 oligomers in living cells. We demonstrate the exchange of TDP-43 between cell somata and the presence of TDP-43 oligomers in microvesicles/exosomes and show that microvesicular TDP-43 is preferentially taken up by recipient cells where it exerts higher toxicity than free TDP-43. Moreover, studies using microfluidic neuronal cultures suggest both anterograde and retrograde trans-synaptic spreading of TDP-43. Finally, we demonstrate TDP-43 oligomer seeding by TDP-43–containing material derived from both cultured cells and ALS patient brain lysate. Thus, using an innovative detection technique, we provide evidence for preferentially microvesicular uptake as well as both soma-to-soma "horizontal" and bidirectional "vertical" synaptic intercellular transmission and prion-like seeding of TDP-43.

Introduction

Amyotrophic lateral sclerosis (ALS) is a neurodegenerative disease affecting primarily cortical and spinal motoneurons, with a fatal outcome resulting from respiratory failure, usually within several years (Pasinelli and Brown, 2006). Motoneuronal deterioration in ALS causes the progressive paresis of voluntarily innervated muscles, which reflects and therefore allows following the neurodegenerative process based on sequential clinical examinations. Even in the earliest descriptions of the disease (Charcot, 1874; Gowers, 1886), not only the progressive nature of ALS symptoms was noted, but also the continuous spreading of clinical motor deficits in ALS patients. This is supported by a more recent systematic description of the distribution of ALS motor deficits by Ravits and La Spada (2009) suggesting a horizontal disease spread to contiguous anatomical regions by transmission of pathology from cell soma to cell soma. In contrast, observations in neuropathological studies in end-stage ALS postmortem tissue were explained by degeneration of motoneurons as a process propagating within the neuroanatomical

systems and suggested a vertical spread of disease pathology (along axons and across synapses; Brettschneider et al., 2014). Using functional magnetic resonance scans and brain functional connectome analysis of patients with different neurodegenerative diseases, including frontotemporal dementia (FTD), Zhou et al. (2012) suggested a trans-neuronal spread model of network-based vulnerability. The dichotomy found in the literature with regard to this topic reflects a controversial discussion about the mode of disease spread, especially about the predominance of either horizontal or vertical spread and the possibility of the coexistence of the two. In addition, vertical spread along axons and across synapses could involve both antero- and retrograde axonal transport.

A systematic progression of neuropathological markers, which correlated with clinical deficits, has been described in detail for Parkinson's disease (Braak et al., 2003). Moreover, a body of evidence has accumulated over recent years, suggesting that the protein α-synuclein may represent the molecular basis for disease spreading in Parkinson's disease (Danzer et al., 2012; Reyes et al., 2014). α-Synuclein is a component of Lewy bodies, cytoplasmic protein aggregates that are

---

*K.M. Danzer and J.H. Weishaupt contributed equally to this paper.

Correspondence to Jochen H. Weishaupt: Jochen.Weishaupt@uni-ulm.de

pathognomonic for this disease. Abundant molecular, cell biological, and genetic evidence points to α-synuclein also being causally involved in disease pathogenesis. α-Synuclein forms oligomers, which can act as seeds for aggregation of α-synuclein monomers (Danzer et al., 2009; Luk et al., 2009). Furthermore, toxic α-synuclein oligomer species can be transmitted intercellularly, thereby constituting a self-perpetuating dissemination of pathology and disease based on a prion-like principle (Goedert et al., 2014; Sato et al., 2014).

It has been speculated that transactive response DNA-binding protein 43 kD (TDP-43) might play an analogous role in ALS. Similar to α-synuclein in Parkinson's disease, aggregated TDP-43 is a pathological hallmark found in most ALS cases, and mutations in the TDP-43 gene *TARDBP* are the cause of ALS in a subset of familial ALS patients (Sreedharan et al., 2008). TDP-43 is a widely expressed, multifunctional RNA-binding protein implicated in various steps of protein coding and non-coding RNA biogenesis (Fiesel and Kahle, 2011; Kawahara and Mieda-Sato, 2012). Under physiological conditions, it is located predominantly in the nucleus. When mutated or under stress conditions, TDP-43 translocates to the cytoplasm, where it participates in the formation of stress granules and eventually becomes hyperphosphorylated and part of insoluble, ubiquitin-positive aggregates typical for the ALS-FTD spectrum of diseases (Neumann et al., 2006, 2009).

Pieces of evidence argue in favor of the hypothesis that TDP-43, similar to toxic α-synuclein species in Parkinson's disease patients, may also be transmitted intercellularly and represent the molecular correlate of infectious systemic disease spreading in ALS (Polymenidou and Cleveland, 2011; Kanouchi et al., 2012). The aggregation-prone TDP-43 protein contains a glycine-rich, intrinsically disordered prion-like domain in its C terminus that could plausibly contribute to disease propagation at the molecular level (Zhang et al., 2009; Budini et al., 2012). From a genetic point of view, it is important to note that almost all ALS- or FTD-causing *TARDBP* mutations cluster within this domain (Pesiridis et al., 2009).

Unfortunately, the detection, characterization, and especially quantification of TDP-43 oligomers using biochemical protocols is hampered by the protein's intrinsic tendency to rapidly form high molecular weight aggregates (Johnson et al., 2009). A recent study based on synthetic peptide fragments of TDP-43 demonstrated the amyloidogenic features of TDP-43, even for the respective wild-type peptide. This study supports the idea that TDP-43 oligomers can be taken up by neurons, induce redistribution of nuclear TDP-43 to the cytoplasm, and therefore lead to toxicity in cells (Zhu et al., 2014), although evidence for toxicity, specifically of the oligomeric form of TDP-43, is still scarce. Furthermore, it was recently shown that MultiFectam-promoted uptake of insoluble TDP-43 induced the formation of similar patterns of insoluble TDP-43 in cells (Nonaka et al., 2013). However, approaches directly demonstrating transmission of cell-derived full-length TDP-43 oligomers without the use of artificial transfection reagents in a live cellular experimental setup are lacking to date.

Here, we developed a highly sensitive and quantitative method for the detection and quantification of total TDP-43 or its oligomeric fraction in living cells based on a protein complementation technique. We demonstrate stress-induced formation of TDP-43 oligomers/aggregates and preferentially microvesicular intercellular spreading of TDP-43. Horizontal spread of TDP-43 could be shown by demonstrating intercellular transmission between human embryonic kidney 293 (HEK-293) cells. Results obtained from neurons cultured in microfluidic chambers further revealed that TDP-43 may be bidirectionally and vertically transmitted across synaptic terminals. Finally, our experimental system allowed the detection of TDP-43 oligomer seeding activity in neurons upon exogenous application of conditioned medium (CM) containing TDP-43 or lysates derived from ALS patient central nervous system (CNS) tissue.

Results

Quantitative detection of TDP-43 oligomers in living cells using a protein complementation approach

We developed a protein complementation technique to quantify TDP-43 dimers/oligomers in living cells. To this end, TDP-43 was fused to the nonbioluminescent N- or C-terminal halves of the humanized *Gaussia princeps* luciferase (constructs named TDP-L1 and TDP-L2, respectively). *G. princeps* luciferase was used instead of firefly luciferase because of its tremendously higher activity and therefore strongly increased assay sensitivity (Tannous et al., 2005). We hypothesized that upon interaction of at least two TDP-43 molecules, preferentially via their prion-like C-terminal domains, luciferase activity would be reconstituted and luminescence could be quantified, representing a measure of TDP-43 dimerization/oligomerization/aggregation (Fig. 1 A). In contrast, to measure total TDP-43, TDP-43 fused to full-length luciferase was used.

In HEK-293 cells cotransfected with TDP-L1 and -L2, a strong luciferase activity could indeed be detected, which was absent in cells cotransfected with the luciferase fragments L1 and L2 only or L1 and TDP-L2 (Fig. 1 C). These results demonstrate that the luciferase tags themselves do not unspecifically self-complement on their own without being attached to TDP-43. To further characterize the TDP-43 oligomer assay, we used size exclusion chromatography (SEC) to separate the different TDP-43 luciferase–active dimers/oligomers/aggregates by their size (Fig. 1, D and E). Luciferase activity was measured, and TDP-43 abundance was determined by dot blot analysis in SEC fractions of TDP-L1– and -L2–cotransfected HEK-293 cells. Under unstressed conditions, we observed a peak of luciferase activity and TDP-43 immunoreactivity in a molecular size range most likely representing physiological TDP-43 dimers (Fig. 1 E).

Cellular stress induces TDP-43 oligomerization

To further characterize our TDP-43 oligomerization assay, we treated cells with sorbitol, which represents an osmotic and oxidative stress paradigm (Dewey et al., 2011). Using our assay, we could confirm that sorbitol treatment of HEK-293 cells leads to nucleocytoplasmic redistribution and accumulation of endogenous TDP-43 in stress granules as well as a shift of this protein to the insoluble cell fraction (Fig. 2, A–C).

Moreover, stress-induced protein aggregation became evident from a prominent high molecular weight total protein peak (280-nm absorbance) in the SEC spectrum of TDP-L1– and -L2–transfected HEK-293 cell lysates upon sorbitol treatment (Fig. 2 D). Luciferase activity measurements of the same SEC fractions revealed a shift of low molecular weight TDP-43 (dimers or small oligomers) to high molecular weight
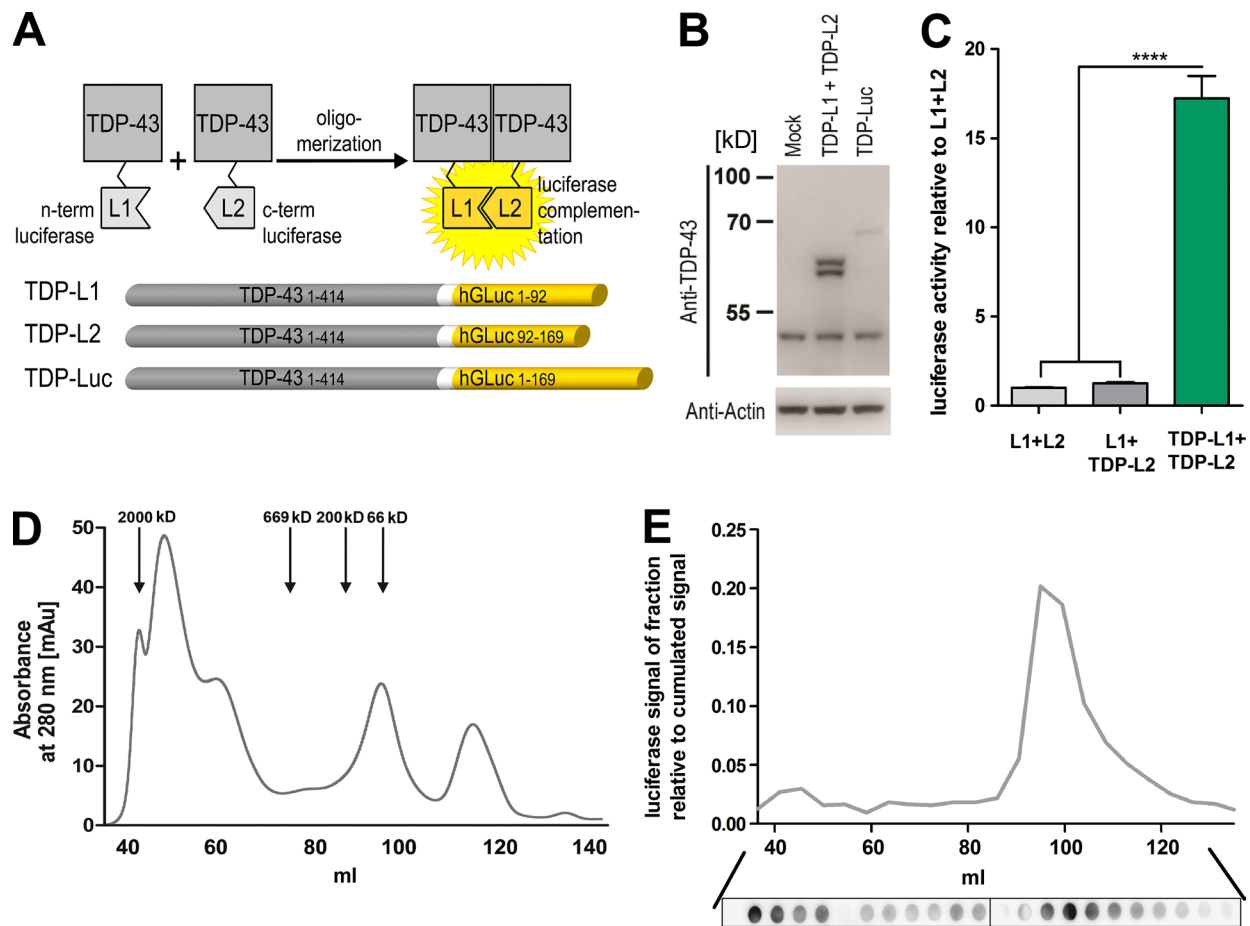
Figure 1. **Quantitative detection of TDP-43 oligomers in living cells using a protein complementation approach.** (A) TDP-43 split luciferase assay principle: oligomerization of TDP-43 monomers fused to nonbioluminescent *G. princeps* luciferase halves (L1 and L2) restores luciferase complementation, which can be quantified. (B) Western blot analysis of TDP-L1 and -L2 coexpression or TDP-Luc expression in HEK-293 cell lysates 48 h after transfection. (C) Luciferase activity measurement in living HEK-293 cells 72 h after cotransfection of either L1 + L2, L1 + TDP-L2, or TDP-L1 + TDP-L2. $n = 10$ per group. Mean ± SEM. ****, $P < 0.0001$. (D) SEC of cell lysates derived from TDP-L1 + TDP-L2–transfected HEK-293 cells. The molecular size standard proteins used were blue dextran (2,000 kD), thyroglobulin (669 kD), β-amylase (200 kD), and BSA (66 kD). (E) Luciferase activity measurement (top) and TDP-43–specific dot blot analysis (bottom) of the same SEC fractions shown in D. The data shown in D and E represent single SEC runs representative for at least three independent repeats.

oligomers/aggregates upon stress induction (Fig. 2 E). The luciferase signal from the TDP-L1/-L2 fusion constructs is thus suitable to demonstrate a shift of TDP-43 oligomers to the high molecular weight fraction of total cellular protein content upon stress. This was accompanied by an increase in the total luciferase signal of TDP-L1– and -L2–transfected HEK-293 cell lysates (Fig. 2 F) as well as a shift of the total TDP-43 content to higher molecular weight SEC fractions, as shown by dot blot analysis (Fig. 2 E). Collectively, our TDP-43 split luciferase constructs proved to be suitable to specifically detect TDP-43 dimers and oligomers and to quantify stress-induced changes in TDP-43 oligomerization and aggregation in living cells.

Intercellular transmission of TDP-43 oligomers

In analogy to the prion-like behavior of α-synuclein in Parkinson's disease (Masuda-Suzukake et al., 2013), intercellular transmission of TDP-43 has been suggested to be the molecular basis for the spreading of symptoms (Ravits and La Spada, 2009) and associated cellular pathology (Brettschneider et

al., 2014) in ALS. We therefore used our TDP-43 oligomerization assay to investigate a possible cell-to-cell transmission of TDP-43. Upon transfection with TDP-L1 and -L2, robust luciferase signal was detected in both HEK-293 cells and the respective culture medium (Fig. 3 A). After culturing nontransfected HEK-293 cells in CM derived from TDP-L1/-L2 (oligomer-derived signal) or TDP-Luc (TDP-43 fused to full-length luciferase, i.e., total TDP-43 signal)–transfected HEK-293 cells for 72 h, luciferase activity could be measured in the recipient cells even after repeated washing (Fig. 3 B). This indicates cellular uptake of total TDP-43 and/or dimers and oligomers, respectively, from the medium. This finding could be confirmed in primary cultures of cortical mouse neurons: cultured neurons were transduced with a rAAV6.2 viral vector harboring TDP-Luc or were cotransduced with rAAV6.2 TDP-L1 and rAAV6.2 TDP-L2. Upon cultivation of naive mouse neurons with respective CM, robust luciferase activity could also be measured in the recipient mouse neurons after an intensive washing procedure (Fig. 3 C). Our luciferase system thus proved neuron-to-neuron transmission of cell-derived full-length TDP-43, at least partially in a dimeric/oligomeric form.
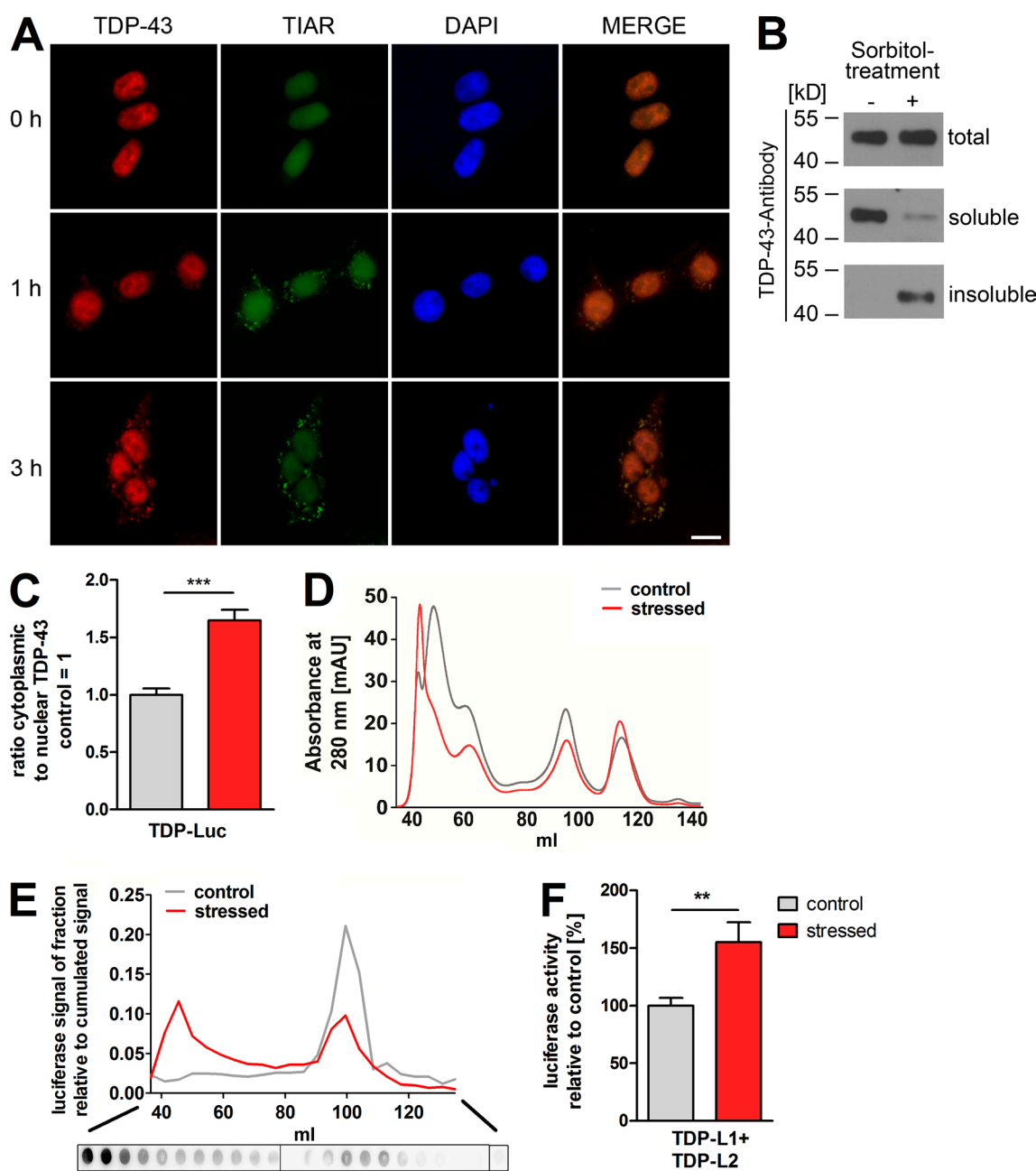
Figure 2. **Detection of stress-induced TDP-43 oligomerization using the luciferase split assay.** (A) Immunofluorescence of endogenous TDP-43 after 400-mM sorbitol treatment in HEK-293 cells at various time points. Stress granules were stained by coimmunolabeling with a TIAR antibody, and nuclei were stained using DAPI. After 1 h of sorbitol treatment, nucleocytoplasmic redistribution of TDP-43 and accumulation in stress granules is observed. Bar, 10 µm. (B) Sorbitol treatment induces the formation of insoluble TDP-43 as assessed by immunoblotting of soluble and insoluble cell lysate fractions. (C) Luciferase activity measurement of nuclear/cytoplasmic fractions of TDP-Luc–transfected HEK-293 cells after 1 h of sorbitol-induced stress. $n = 11$ per group. (D) SEC of cell lysates derived from TDP-L1 + TDP-L2–transfected HEK-293 cells after sorbitol-induced stress. Absorbance at 280 nm shows the size distribution of the total protein content. (E) Luciferase activity measurement (top) and TDP-43–specific dot blot analysis (bottom) in the SEC fractions of stressed HEK-293 cells in D. (F) Total luciferase activity measurement in living HEK-293 cells expressing TDP-L1 and TDP-L2 with or without sorbitol stress. $n = 20$ per group. Mean ± SEM. **, $P < 0.01$; ***, $P < 0.001$. The data shown in D and E represent single SEC runs representative for at least three independent repeats. mAU, milli absorbance units.

Preferential uptake and toxicity of microvesicular/exosomal TDP-43

There are several possible intercellular transmission pathways for proteins, for example as a secreted free protein or packaged in vesicular bodies such as microvesicles/exosomes (MVEs). As exosomal transfer has already been shown to be relevant in other neurodegenerative diseases, e.g., transmission of toxic α-synuclein oligomers in Parkinson's disease models (Danzer et

al., 2012), we sought to investigate whether TDP-43 can also be transmitted by MVEs. To this end, HEK-293 cells were transfected with myc-tagged TDP-43, and MVEs were prepared 72 h later. To demonstrate the purity of the MVE fraction, we first examined the MVEs for the presence of the exosomal markers flotillin-1, CD-63, and the absence of contaminating cell organelles such as mitochondria, endoplasmic reticulum (Bcl-2), and Golgi apparatus (GM130; Fig. S1 A). Transmission EM (TEM)
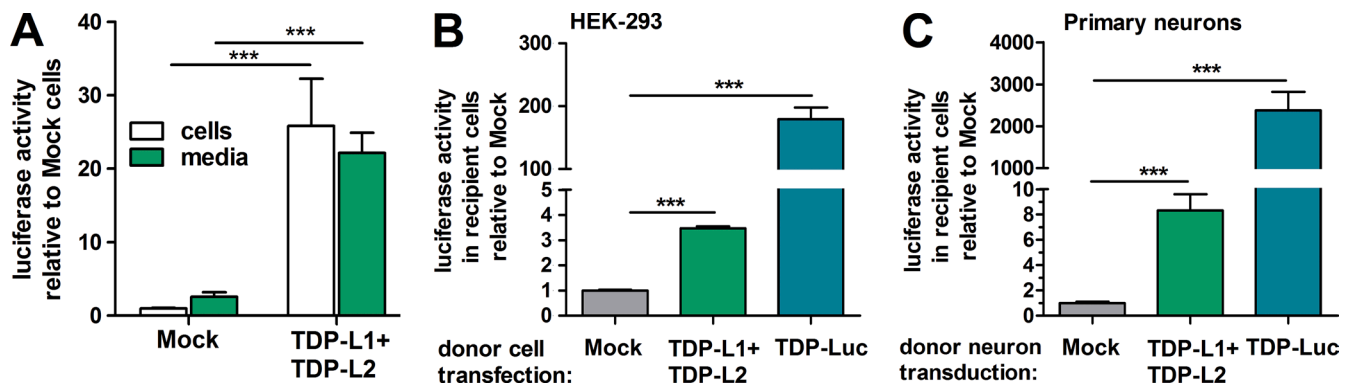
Figure 3. **Intercellular transmission of TDP-43 oligomers.** (A) Luciferase activity measurement of intact cells and CM from HEK-293 cells cotransfected with TDP-L1 + TDP-L2. n = 20. (B) Luciferase activity measurements after extensive washing of naive HEK-293 cells cultured for 72 h in CM. CM was obtained from HEK-293 cells transfected either with mock, TDP-L1 + TDP-L2, or TDP-Luc. n = 4 per group. (C) Luciferase activity measurements of naive primary cortical mouse neurons cultured for 72 h in CM. CM was obtained from primary neurons transduced with rAAV6.2 encoding TDP-L1 + TDP-L2 or TDP-Luc. n = 12 per group. Mean ± SEM. ***, P < 0.001.

of ultrathin sections of the MVEs further confirmed the presence of intact vesicles with lipid bilayer membranes (Fig. 4 A). Characterization of the MVEs by nanosight measurements showed a depletion of MVE-sized particles in the MVE-free supernatant compared with the CM before ultracentrifugation (Fig. S1 B). Furthermore, the mode of particle size of the MVEs is in accordance with previously published results of HEK-293–derived MVEs (Fig. S1, C and D; Chernyshev et al., 2015). In agreement with recent biochemical and mass spectrometry data of endogenous TDP-43 (Feneberg et al., 2014), immunogold-TEM of our MVEs clearly proved the presence of TDP-43 in the lumen of microvesicles (Fig. 4, B and C). Interestingly, in addition to intraluminal localization of TDP-43, we further detected MVE-membrane–associated TDP-43 (Fig. 4 D). Additionally, Western blot analysis confirmed the presence of both endogenous TDP-43 and myc–TDP-43 in MVEs of myc–TDP-43–transfected HEK-293 cells (Fig. 4 E). Moreover, robust luciferase activity in MVEs from TDP-Luc– but also TDP-L1/-L2–transfected cells demonstrated that MVE-packaged TDP-43 comprises a dimeric/oligomeric subfraction (Fig. 4 F). Notably, luciferase alone without being fused to TDP-43 was not targeted to MVEs (Fig. 4 F), indicating that MVE targeting was specific for TDP-43 and not promoted by the luciferase tag. Furthermore, we observed that MVE-packaged TDP-43 was taken up much more efficiently than non-MVE–packaged free TDP-43 by both naive HEK-293 cells (Fig. 4 G) and cultured primary neurons (Fig. 4 H). In addition, this increase in cellular uptake of TDP-43 also translated into higher toxicity in recipient neurons, as shown by caspase-3/7 measurements, where MVE-packaged TDP-43 exerted higher toxicity than did equal amounts of non-MVE–packaged TDP-43 (Fig. 4 I).

TDP-43 is taken up and transmitted by axon terminals

We have shown that toxic subfractions of TDP-43 can be transmitted between neurons. Recent neuropathological studies of ALS patient postmortem brains (Brettschneider et al., 2014) described a pattern of phospho–TDP-43 immunoreactivity that is in agreement with a systematic spread of TDP-43 pathology between distant locations in the CNS by axonal transport and finally transmission across synapses. To investigate the possible uptake and transmission of TDP-43 by axon terminals, we thus used a compartmentalized microfluidic culture system, which allowed us to culture neuronal cell bodies fluidically isolated from

their axon terminals (Fig. 5, A and D). Primary mouse cortical neurons were cultured in the microfluidic system and transduced with the rAAV6.2 viral vector encoding TDP-Luc at day in vitro (DIV) 5. TDP-Luc was used instead of TDP-L1/-L2 constructs to ensure that sufficient traceable luciferase signal was present upon transduction to allow studying vertical transmission. 24 h later, neuronal H4 cells were plated in the fluidically separated axonal chamber (Fig. 5 A). After 5 d of co-culture, luciferase activity was detected in the H4 cells (Fig. 5 B), indicating that TDP-43 was transmitted from the neuronal terminals to H4 cells. To prevent passive diffusion of TDP-Luc, excess medium was added to the chamber in which the H4 cells were cultured. Importantly, luciferase signal could only be detected in the H4 cells when primary neurons had been seeded in the opposite chamber (Fig. 5 C), indicating that neuronal axons and their terminals were required to transmit TDP-Luc. We next tested whether TDP-43 could also be transmitted retrogradely, i.e., taken up by axon terminals and transported to neuronal somata in the opposite chamber. CM from cells overexpressing TDP-Luc was added to the axon terminals (Fig. 5 D). After 5 d, luciferase activity was detected in the lysates of neuronal somata in the opposite chamber, indicating that neurons had taken up TDP-43 by axon terminals and transported it retrogradely (Fig. 5 E). Luciferase activity was not above background value in this chamber when neuronal cells were omitted (Fig. 5 F). When the CM was derived from cells expressing luciferase not fused to TDP-43, retrograde transmission of luciferase activity from one chamber to the recipient neuronal somata in the other chamber was hardly above background level (Fig. 5 E), indicating a TDP-43–dependent process. These findings show that neurons are able to both transmit TDP-43 anterogradely from axon terminals to subsequent cell populations and to take up TDP-43 by axonal terminals followed by retrograde transport to the soma.

Transmitted and target cell–derived TDP-43 interact and are found in the same cytoplasmic granule

Having shown that TDP-43 can be transmitted intercellularly, we next studied whether uptaken TDP-43 is able to interact with the endogenously expressed TDP-43 of the recipient cell. First, we confirmed that transfected TDP-L1 and -L2 could principally interact with endogenous TDP-43. To this end, immunoprecipitation from cell lysates using a polyclonal luciferase
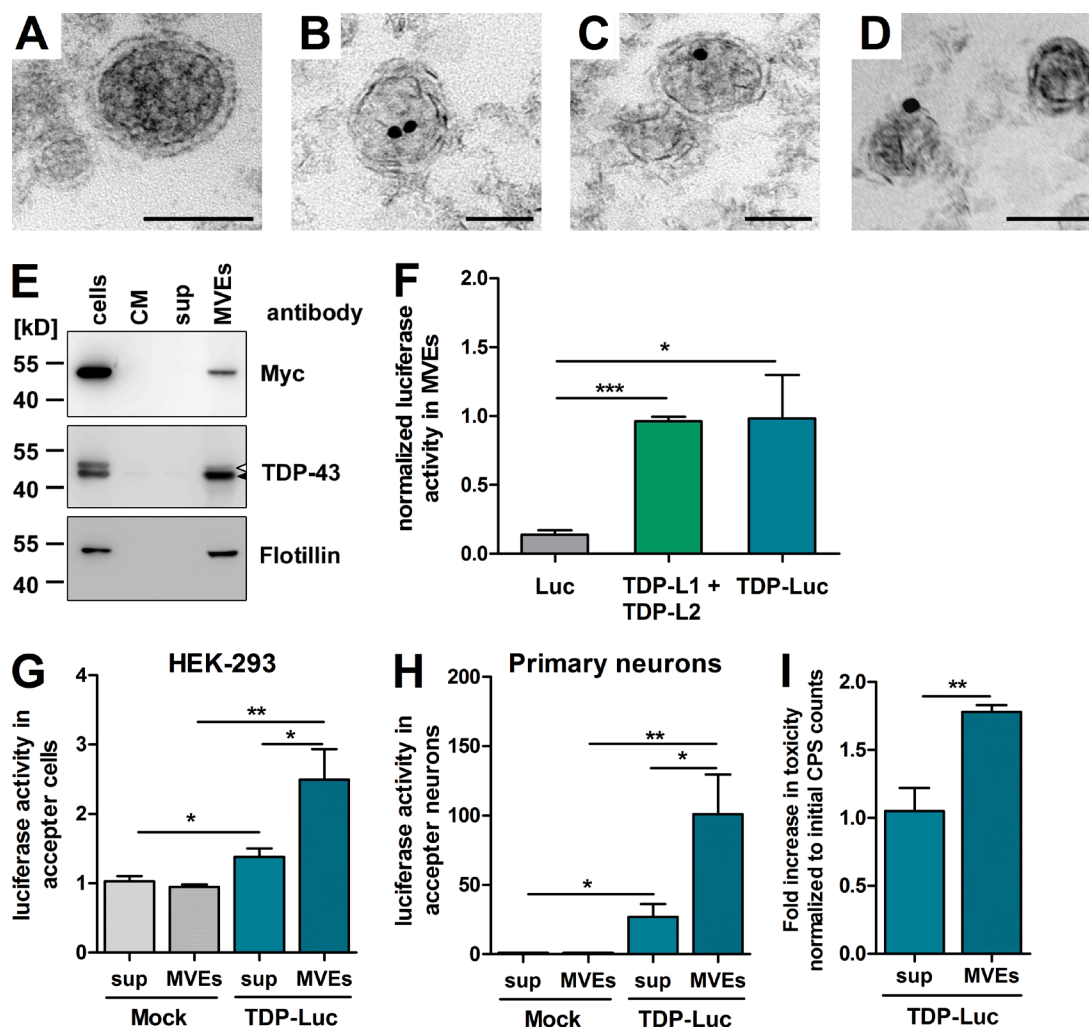
Figure 4. **Preferential uptake and higher toxicity of microvesicular/exosomal TDP-43.** (A) TEM pictures of ultrathin sections of MVEs. A representative micrograph of intact vesicles with a bilayered lipid membrane is shown. (B–D) Anti–TDP-43 immunogold labeling was performed on ultrathin sections of MVEs (10-nm gold particles). Intraluminal (B and C) and membrane-associated (D) TDP-43 is shown. Bars, 50 nm. (E) Immunoblotting of HEK-293 cells transfected with myc–TDP-43 and their corresponding CM MVE-free supernatant after ultracentrifugation (sup) and MVEs. Overexpressed myc–TDP-43 was detected using a Myc antibody, and endogenous TDP-43 was detected in MVEs using a TDP-43 antibody. Flotillin was used as an MVE marker. The closed arrowhead indicates endogenous TDP-43, and the open arrowhead indicates myc–TDP-43. (F) MVEs were prepared from HEK-293 cells expressing either full-length luciferase alone (Luc), TDP-L1 + TDP-L2, or TDP-43 fused to full-length luciferase (TDP-Luc). Luciferase activity of MVE fractions was normalized to the activity measured in the respective host cells. $n = 12$ per group. (G and H) MVE fractions (MVEs) and MVE-free supernatants (sup) from HEK-293 cells transfected with control vector (Mock) or TDP-Luc were applied to naive HEK-293 cells (G) or primary neurons (H) and incubated for 3 d. Uptake of TDP-Luc was detected by luciferase activity measurement. $n = 14$. (I) Caspase-3/7 toxicity assay of naive primary neurons treated with MVE fraction (MVEs) or MVE-free supernatant (sup) containing TDP-Luc. $n = 9$ per group. Mean ± SEM. *, $P < 0.05$; **, $P < 0.01$; ***, $P < 0.001$. CPS, counts per second.

antibody was followed by Western blot analysis using a TDP-43 antibody. We found that endogenous, untagged TDP-43 was co-immunoprecipitated with TDP-L1/-L2 expressed by DNA vector transfection of the same cell (Fig. 6 A). To prove direct interaction of TDP-43 taken up from outside the cell with endogenously synthesized TDP-43, we used an additional split protein technique. To that end, N-terminal or C-terminal fragments of the fluorescent protein VenusYFP are fused to TDP-43 (TDP-V1 and TDP-V2; Fig. 6 B). Similar expression levels and stability of the two fusion constructs were confirmed by Western blotting (Fig. S2 A). Each TDP-43-split-VenusYFP fusion protein alone completely lacked fluorescence as a result of disruption of the chromophore, whereas cotransfection of both constructs resulted in robust fluorescence (Fig. S2 B). We next transfected separate cultures of HEK-293 cells with either the TDP-V1 or TDP-V2 construct. 2 d later, the separately transfected cell cultures were

trypsinated, thoroughly washed, and then coplated and cultured in one dish for another 2 d (Fig. 6 C). After the additional 2 d, reconstitution of the VenusYFP fragments was indicated by distinct cytoplasmic VenusYFP fluorescence in a subset of the cocultured cells (Fig. 6 D). This observation indicated that TDP-V1 and TDP-V2 were exchanged between cells, and direct interaction of the two different TDP-V1/-V2 fusion proteins, originally expressed in separate cell cultures, must have occurred.

Assuming that TDP-43 taken up from the extracellular space may be involved in seeding cytoplasmic TDP-43 deposits, we tested whether exogenously uptaken and endogenously present TDP-43 can be found in the same cytoplasmic granules. Therefore, the CM from HEK-293 cells transfected with TDP-43–full-length–VenusYFP (TDP-Venus) was added to naive cells. These cells were then stressed by sorbitol to enhance stress granule formation, which has been proposed to be a possible
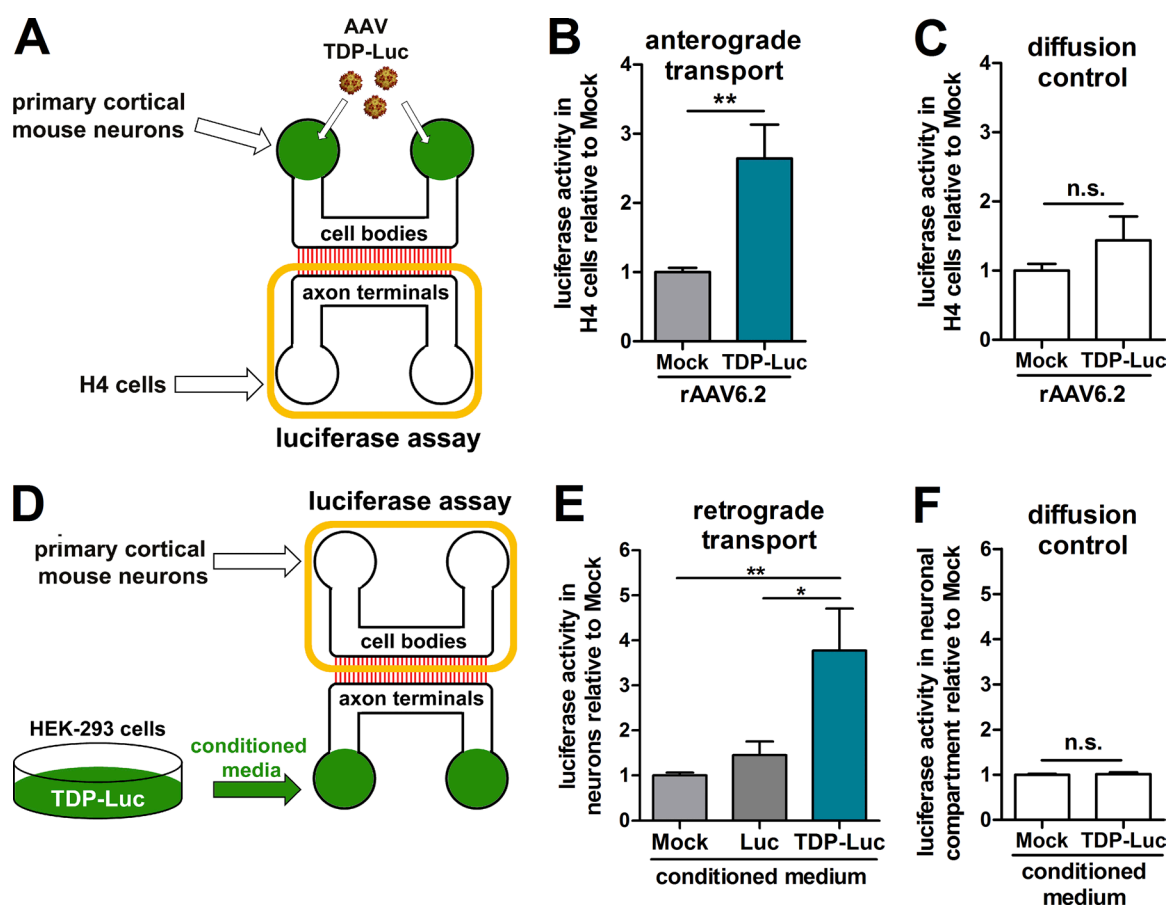
Figure 5. **Axonal uptake and transmission of TDP-43.** (A) Experimental design of the anterograde transmission experiment. (B) Primary cortical mouse neurons in microfluidic devices (5 DIV) were transduced with rAAV6.2 TDP-Luc. After 24 h, H4 cells were coplated in the axonal terminal compartment. Excess culture medium was added to the axonal compartment during the entire experiment to maintain a positive hydraulic pressure and prevent diffusion of TDP-43 or virus particles. After 5 d of co-culture, H4 cells were harvested, and luciferase activity was detected. (C) The same setup without primary neurons was used as a diffusion control. (D) Experimental design of the axon terminal uptake experiment. (E) CM from HEK-293 cells transfected with mock, Luc, or TDP-Luc were added to the axonal compartment of microfluidic devices containing primary cortical neurons (5 DIV). Excess culture medium was added to the cell body compartment to maintain a positive hydraulic pressure against protein diffusion during the entire experiment. After 5 d, neuron bodies were harvested, and luciferase activity was measured. (F) The same setup without primary neurons was used as a diffusion control. For all experiments, n = 9. Mean ± SEM. *, P < 0.05; **, P < 0.01. Yellow rectangles in A and D indicate compartments from which cell bodies were harvested for luciferase activity measurement in the respective experiment. n.s., not significant.

first step in TDP-43 aggregate deposition in ALS (Maniecka and Polymenidou, 2015), followed by immunostaining for total TDP-43 and analysis by confocal microscopy (Fig. 6 E). Z-stack imaging analysis identified cells with cytoplasmic granules with a core that contained VenusYFP-tagged TDP-43 taken up from the CM (both green Venus signal and red TDP-43 immunostaining signal), which was surrounded by endogenously produced TDP-43 (solely red signal; Fig. 6 F). This experiment demonstrates that uptaken and endogenous TDP-43 can participate in the formation of the same cytoplasmic TDP-43 granule. TDP-43 taken up from outside the cell, most likely together with endogenous TDP-43, was part of the granule core, and therefore likely involved in the first steps of granule formation.

Cell culture–derived TDP-43 and ALS patient–derived CNS lysates induce TDP-43 oligomerization in recipient cells

Our finding that TDP-43 can be transmitted intercellularly and across neuronal terminals is in agreement with the hypothesis of a prion-like transmission of TDP-43 pathology. Furthermore,

as a prerequisite for a possible prion-like seeding, we proved the interaction of exogenous, uptaken TDP-43 and TDP-43 endogenously expressed by the target cell. Therefore, we next asked whether exogenous TDP-43 could indeed trigger TDP-43 oligomerization in recipient cells. To address this question, we cultured HEK-293 cells cotransfected with TDP-L1 and -L2 constructs in CM derived from either myc–TDP-43– or mock-transfected HEK-293 cells. We found that the presence and uptake of TDP-43 from the medium triggered oligomerization of TDP-43 expressed in the recipient HEK-293 cells (Fig. 7 B). Similar results were obtained when primary cortical mouse neurons were used (Fig. 7 C). Finally, we tested whether CNS lysates from ALS patients, which had a confirmed TDP-43 pathology, could induce TDP-43 oligomerization in our cellular assay. To this end, natively frozen cerebellum and cortex samples of ALS patients and gender- and age-matched healthy controls (Table 1) were homogenized and centrifuged. 3 d after transduction of mouse primary neurons with TDP-L1/-L2 rAAV6.2 vectors, CNS lysate pellets were resuspended in PBS, adjusted to equal protein concentrations, and added to the
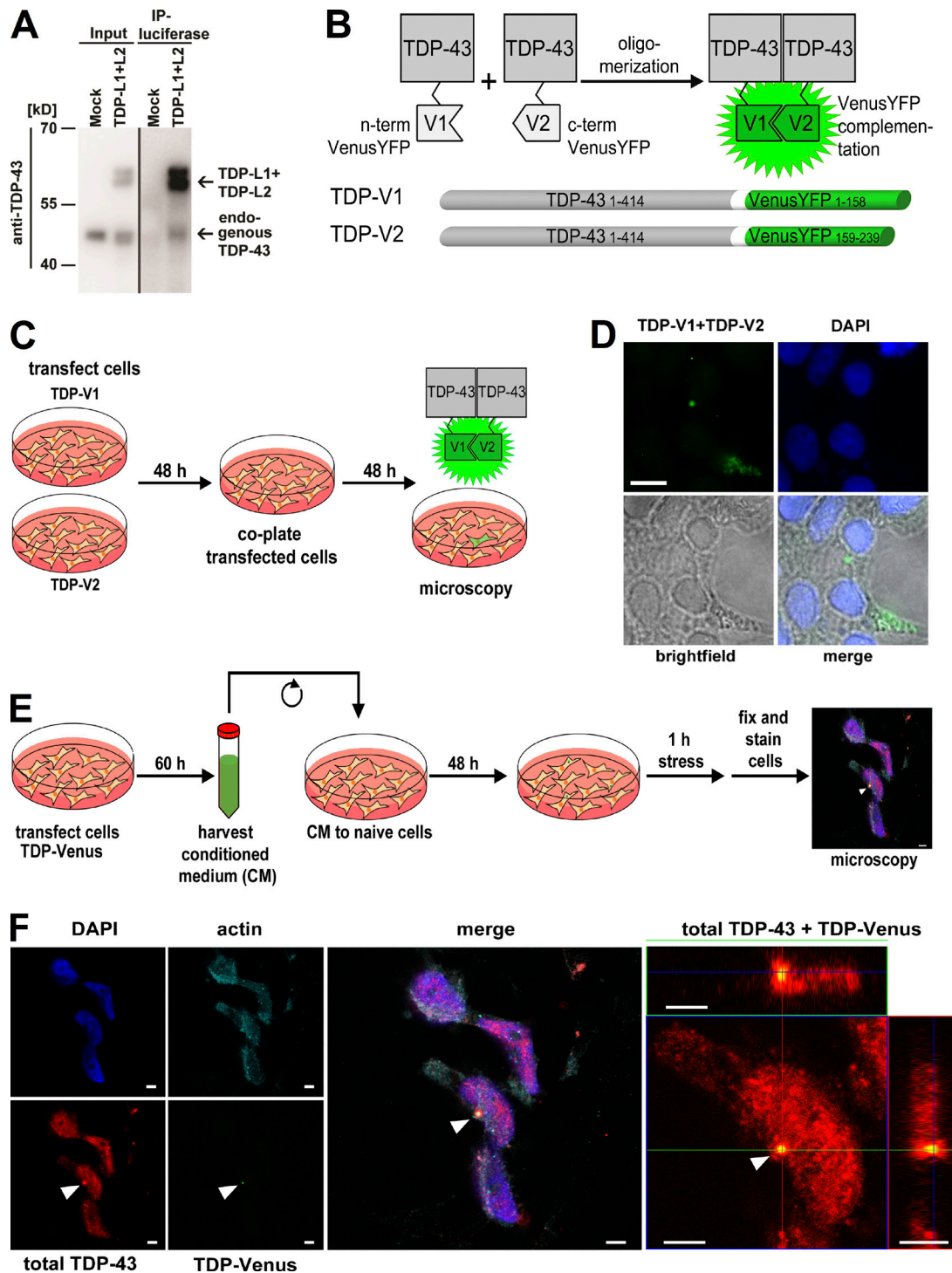
Figure 6. **Transmitted and target cell–derived TDP-43 interact and are found in the same cytoplasmic granule.** (A) Coimmunoprecipitation of overexpressed TDP-L1 + TDP-L2 and endogenous TDP-43 using a polyclonal luciferase antibody demonstrates that the transfected TDP-L1 and TDP-L2 constructs interact with endogenous TDP-43 in HEK-293. Cell lysate of HEK-293 cells transfected with an empty vector (mock) was used as a negative control. One representative Western blot of three replicates is shown. (B) TDP-43 split VenusYFP assay principle and constructs are shown. Oligomerization of TDP-43 monomers fused to nonfluorescent VenusYFP halves (V1 and V2) restores VenusYFP fluorescence, which is visualized by microscopy. (C) Setup for the co-culture experiment using the VenusYFP split constructs. (D) Fluorescence micrographs of co-culture experiment. After 48 h of co-culturing, HEK-293 cells originally transfected with either TDP-V1 or TDP-V2 VenusYFP-positive cells were detected. Cell nuclei were stained with DAPI. Bar, 10 μm. (E) Setup for uptake experiment using TDP full-length Venus (TDP-Venus), followed by sorbitol stress (400 mM for 1 h) and immunostaining for TDP-43. The arrowhead indicates an aggregate. Bar, 5 μm. (F) Representative micrograph of a cell that took up TDP-Venus (green) from CM. After stressing the cell with sorbitol, total TDP-43 (red) and α–smooth muscle actin (cyan) were immunolabeled, and nuclei were stained with DAPI. Arrowheads indicate an aggregate with a core containing TDP-Venus (green; labeled also by the total TDP-43 immunostaining in red) surrounded by a solely red immunostaining signal, indicating endogenously expressed, untagged TDP-43. (Right) Orthogonal projections of confocal z stacks of the aggregate-containing cell. Bars, 5 μm. IP, immunoprecipitation.

Table 1.   Human CNS tissue samples

Tissue	Group	n	Gender	Age (mean ± SD)
Cerebellum	Controls	9	7 males; 2 females	64.0 ± 13.6
	ALS patients	9	8 males; 1 female	66.1 ± 12.0
Cortex	Controls	8	6 males; 2 females	66.4 ± 12.5
	ALS patients	8	7 males; 1 female	65.9 ± 12.8

culture medium. Luciferase activity was measured after 4.5 h. No difference in luciferase activity was detected between cerebellum-derived lysates from patients and controls (Fig. 7 D). In contrast, cortex-derived patient samples, in which TDP-43 pathology is highly abundant, induced TDP-43 oligomerization in cultured neurons (Fig. 7 E). Thus, patient-derived tissue lysate of a CNS region that represents a primary site of TDP-43 pathology in ALS triggered TDP-43 oligomerization in our neuronal in vitro assay.

Discussion

Here, we developed an innovative split protein technique to quantitatively detect TDP-43 dimers and oligomers in living neurons. We demonstrate the neuronal release and uptake of TDP-43 as well as its seeding and toxic activity in recipient cells. Furthermore, we delineate the mode and neuronal compartment involved in TDP-43 transmission.

We have established the first assay that allows quantifying TDP-43 dimerization/oligomerization in living cells. It is based on fragments of the *G. princeps* luciferase, which is superior to the widely used firefly luciferase because of a tremendously increased activity and therefore sensitivity (Tannous et al., 2005). Fragments of the luciferase are fused to the C terminus of TDP-43 and reconstitute an active enzyme as soon as TDP-43 forms oligomers, a principle that was adopted from previous studies using split luciferase/α-synuclein fusion constructs (Remy and Michnick, 2006) to study α-synuclein oligomerization (Outeiro et al., 2008; Danzer et al., 2011, 2012). Our split luciferase system was able to detect the expected stress-induced increase in TDP-43 oligomerization in living HEK-293 cells. Results from SEC further validated our TDP-43 oligomerization assay.

Although mutant TDP-43 is known to be associated with rare familial forms of ALS, our study focused on the transmission of wild-type TDP-43. This direction of our work was based on the fact that TDP-43 aggregates are found in most ALS cases, both familial and sporadic forms. Moreover, wild-type full-length TDP-43 itself already has a high propensity to form aggregates (Zhu et al., 2014), has been suggested to correlate with histopathological disease spreading in ALS patients (Brettschneider et al., 2014), and induced motor deficits and
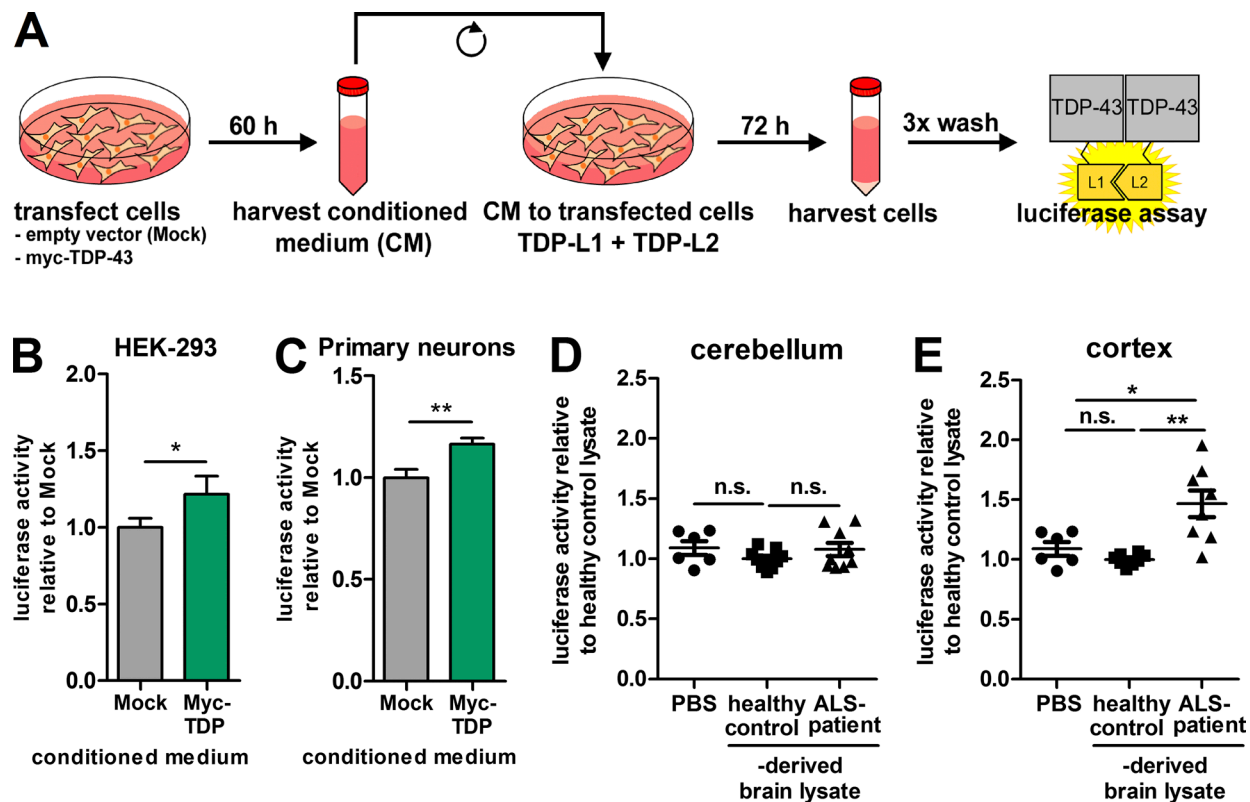

Figure 7.   TDP-43 oligomer seeding in recipient cells induced by cell culture material and ALS patient–derived CNS lysates. (A) Setup for seeding experiments with CM. (B and C) Luciferase activity measurement 3 d after CM from HEK-293 cells transfected with mock or myc-TDP was added to either HEK-293 cells cotransfected with TDP-L1 + TDP-L2 (B) or primary mouse neurons cotransduced with rAAV6.2 encoding TDP-L1 and TDP-L2 (C). $n = 14$ and $n = 27$, respectively. (D and E) Luciferase activity measurement of mouse primary neurons cotransduced with rAAV6.2 encoding TDP-L1 and TDP-L2 after 4.5 h of treatment with postmortem cerebellar ($n = 9$ different patients and controls) or cortical ($n = 8$ different patients and controls) lysates, respectively. Mean ± SEM. *, $P < 0.05$; **, $P < 0.01$. n.s., not significant.

earlier lethality upon overexpression in transgenic mouse models (Tsai et al., 2010; Wils et al., 2010; Xu et al., 2010).

As we use full-length TDP-43 for our studies, it is also important to note that in the postmortem situation, the TDP-43 antibodies commonly used for neuropathology stain large cytoplasmic aggregates containing truncated and also hyperphosphorylated TDP-43. However, it is an ongoing debate whether the large, phosphorylated inclusions, which are visible by conventional light microscopy, are still involved in the disease progression or represent inert end-stage or even protective aggregates. Sporadic ALS patients with an unusually long disease course showed a relatively low number of neurons bearing phosphorylated TDP-43 inclusions compared with patients with a more rapid disease progression (Nishihira et al., 2009). A possible interpretation of this finding is that neurons harboring TDP-43 inclusions are more prone for neurodegeneration. In contrast, studies in mice demonstrated that light microscopically visible TDP-43 aggregation is not an absolute requirement for TDP-43–induced neurodegeneration (Igaz et al., 2011). Brettschneider et al. (2014) found aggregated and phosphorylated TDP-43 in the neuronal somata of affected cells, but not in the axons of neurons that possibly transmit TDP-43 vertically to their target neurons. Overall, these findings suggest oligomeric TDP-43, which does not form aggregates visible by conventional light microscopy, as a plausible candidate for toxicity and prion-like disease spreading in ALS patients.

We were able to demonstrate transfer of cell-derived full-length TDP-43 between neurons. This represents a possible molecular correlate for the clinically observed spreading of ALS disease symptoms from a focal site of onset, as mentioned already in early descriptions of ALS by Charcot (1874) and Gowers (1886) and systematically characterized just a few years ago (Ravits and La Spada, 2009). Our findings are also principally in agreement with a neuropathological study of ALS postmortem tissue, which demonstrated a gradient of cytoplasmic, pathological TDP-43 aggregates between separate brain areas (Brettschneider et al., 2014). Based on neuropathological findings in Alzheimer's and Parkinson's disease patient tissue (Braak and Braak, 1991; Braak et al., 2003), it has been hypothesized earlier that intrinsically unfolded, aggregation-prone proteins adopt prion-like properties. They are transmitted between cells and further propagate protein oligomer/aggregate formation in the target cells (Meyer-Luehmann et al., 2006; Luk et al., 2012). For α-synuclein and tau, a considerable body of evidence exists already to support this hypothesis, whereas our study provides the first cell biological data to extend this concept to TDP-43.

We were able to detect TDP-43 oligomer seeding activity of both cell culture–derived material and neuropathologically affected human ALS CNS lysates and show that intercellularly transmitted TDP-43 participates in TDP-43 granule formation in target cells. Our data are thus in line with data by Nonaka et al. (2013), who recently demonstrated TDP-43 seeding in a self-templating manner. However, these results were obtained using MultiFectam transfection reagent (Promega) to promote TDP-43 uptake into recipient cells, whereas our study abstains from using such enhancing reagents, thereby representing a far more physiological experimental approach. From a technical perspective, we provide a quantitative assay that is suitable to measure TDP-43 seeding activity or "infectivity" for other research or may even be developed for clinical diagnostic purposes.

Furthermore, our finding that TDP-43–Luc, but not the luciferase tag alone, was detected in highly purified MVEs indicates a specific TDP-43 MVE targeting. This finding was confirmed using immunogold labeling of TDP-43 in conjunction with TEM. The presence of TDP-43 within MVEs was shown in ultrathin sections of pressure-frozen and embedded MVEs. These data delineate a likely route for how TDP-43 is shuttled to other cells. Moreover, we showed that TDP-43 packaged in MVEs is preferentially taken up by target cells, i.e., both HEK-293 cells and neurons, compared with TDP-43 present in the MVE-free medium preparation. These results are highly reminiscent of a recent study demonstrating cell-to-cell transmission of toxic α-synuclein oligomers by exosomes (Danzer et al., 2012). Our data therefore support the concept of MVEs as intercellular carriers of toxic protein oligomers in the context of several different neurodegeneration-related proteins and diseases.

Spreading of histopathology in ALS may occur "horizontally," i.e., from one cell body to another, or follow "vertical" anatomical and functional structures linking separated brain areas by axonal connection (Braak et al., 2013). A recent neuropathological study in ALS postmortem material favors the latter possibility, as TDP-43 pathology was observed in distant brain regions that are axonally connected (Brettschneider et al., 2014). Partially in support of this view, we observed somatic uptake, anterograde axonal transport, and even vertical transmission of TDP-43 to post-terminal cells in a cell culture chamber that fluidically separates neuronal somata from axon terminals/synapses. In addition to an anterograde transport and transmission, we also observed efficient uptake of TDP-43 by axon terminals and retrograde transport to the neuronal somata. This contradicts a solely anterograde (corticofugal), vertical spreading hypothesis raised by postmortem studies (Brettschneider et al., 2013, 2014). Because of the early fatal outcome of ALS, current neuropathological studies represent only the end-stage situation. Therefore, several different models are conceivable that can explain the vertical (corticofugal) phospho–TDP-43 aggregate gradient pattern observed in postmortem ALS brains. This includes, for instance, a combination of antero- and retrograde transport of TDP-43 or even a multiphasic sequence of aggregation and partial resolution of cytoplasmic TDP-43 aggregates in different brain regions. Furthermore, a bidirectional transmission of TDP-43 could explain the complex variable distribution of the disease between upper (cortical) and lower (spinal) motoneuron onset in ALS patients. Ultimately, horizontal (contiguous) spread in the extracellular space (from cell soma to cell soma), as also observed in our experiments, together with variable vulnerabilities of neuronal subtypes, might also explain the neuropathological observations by Brettschneider et al. (2014), or even coexist with a vertical (axonal) spreading. Interestingly, an elegant study showed transmission and terminal uptake of synthetic peptides corresponding to fragments of wild-type and mutant TDP-43 (Zhu et al., 2014), which is in agreement with results from our approach based on cell-derived full-length TDP-43.

In summary, we established an assay for the detection of TDP-43 seeding activity in cell culture or ALS patient postmortem biomaterial. Application of our innovative method provides experimental evidence for interneuronal, bidirectional vertical trans-synaptic spreading of TDP-43 and also for horizontal transmission between cell somata that might occur in part via microvesicular transport. Both TDP-43 oligomers themselves and respective mechanisms of transmission represent potential new therapeutic targets.

Materials and methods

Plasmids

Fusion constructs contain a cytomegalovirus promoter and are based on pcDNA3.1-Zipper-hGluc(1) and pcDNA3.1-Zipper-hGluc(2) (Remy and Michnick, 2006) used for detection of α-synuclein oligomer (Outeiro et al., 2008). α-Synuclein was replaced by TDP-43 using EcoRV–ClaI sites. Fusion construct TDP-43–Luc was created by cloning the humanized *G. princeps* luciferase with a linker into the EcoRI–XhoI sites of pcDNA3. TDP-43 was subsequently cloned into the BamHI site. For the VenusYFP constructs, α-synuclein (Danzer et al., 2011) was replaced by TDP-43 using BamHI–EcoRV sites. Fusion construct TDP-43–Venus was created by cloning the VenusYFP with a linker into the EcoRV–XhoI sites of pcDNA3. TDP-43 was subsequently cloned into the BamHI–EcoRV sites. The Myc–TDP-43 construct was provided by D. Dormann (Ludwig Maximilian University of Munich, Munich, Germany).

AAV vectors

Plasmids for the production of recombinant adeno-associated vectors rAAV-TDP-L1, rAAV-TDP-L2, and rAAV-TDP-Luc were constructed by cloning TDP-L1 and TDP-L2 into XhoI–EcoRV sites of the AAV-CBA-WPRE vector. TDP-Luc was cloned into the EcoRI–XhoI sites of the AAV-CBA-WPRE vector. The AAV6.2 cap gene was synthesized (Life Technologies) and cloned into pAAV-RC (Agilent Technologies), thereby replacing the AAV2 cap gene. AAV vectors were produced in HEK-293 cells using the AAV helper-free system (Agilent Technologies) and purified as described previously (Strobel et al., 2015). In brief, HEK-293 cells were cotransfected with the plasmid encoding AAV6.2, pHelper (AAV helper-free system), and the rAAV plasmid harboring the TDP-43 construct of interest. After 3 d of growth, cells were detached, resuspended in 50-mM Tris, 150-mM NaCl, and 2-mM $MgCl_2$, pH 8.5, and lysed by three freeze/thaw cycles before benzonase nuclease (Merck) was added to digest DNA. After pelleting cell debris by centrifugation, the AAV-containing supernatant was overlaid onto an iodixanol density gradient, consisting of 8 ml of 15%, 6 ml of 25%, 8 ml of 40%, and 5 ml of 58% iodixanol (Sigma-Aldrich) diluted in PBS-MK (1× PBS, 1-mM $MgCl_2$, and 2.5-mM KCl). The 15% phase additionally contained 1-M NaCl. After 2 h of centrifugation at 63,000 rpm using a rotor (70 Ti; Beckman Coulter), 4 ml of the lower part of the 40% phase were isolated for AAV recovery. After dialysis/concentration using ultrafiltration devices (Amicon-15; EMD Millipore), AAV vectors were formulated in PBS + 10% glycerol, sterile filtrated, and stored at −80°C.

Cell culture maintenance, transfection, and stress

HEK-293 cells were maintained in DMEM containing 10% FCS (both from Life Technologies) at 37°C and 5% CO_2. Cells were plated 24 h before transfection and were transfected using calcium phosphate precipitation. The split constructs (TDP-L1 and -L2) were transfected using equimolar ratios. Transfection medium was replaced after 12 h, and CM was collected after an additional 60 h and centrifuged at 3,000 g for 5 min to eliminate floating cells. Sorbitol was used as a stressor at 400 mM in DMEM + 10% FCS for 1 h unless otherwise stated.

Primary cortical neuron cell culture

Primary cortical neurons were prepared from cerebral cortices of embryonic day (E) 15 mouse embryos (C57BL/6J). Cortices were dissected from embryonic brain, meninges were removed, and cortices were resuspended in neurobasal medium (Life Technologies) supplemented with 2-mM GlutaMAX, 100 U/ml penicillin, and 2% (vol/vol) B-27. The cells were plated at a density of 40,000 cells/well on a 96-well plate and 1,000,000 cells/well on 60-mm dishes. All wells/dishes were previously coated with 10 µg/ml poly-D-lysine (Sigma-Aldrich). Every third day, 50% of the medium was replaced.

Luciferase assay

HEK-293 cells were transfected in a 96-well plate. 16 h after transfection, medium was replaced by serum- and phenol red–free DMEM. 72 h after transfection, medium was transferred to a new 96-well plate for luciferase activity measurement of secreted protein. Cells were washed with PBS, and new serum- and phenol red–free medium was added for luciferase activity measurement. Luminescence was detected using an automated plate reader at 480 nm after the addition of the cell-permeable substrate coelenterazine (40 µM; PJK GmbH), with a signal integration time of 2 s.

SEC

HEK-293 cells were cotransfected with TDP-L1 and TDP-L2 plasmids. 48 h after transfection, cells were washed twice with PBS and lysed in PBS using sonication. Protein concentration was detected using a bicinchoninic acid (BCA) protein assay, and a concentration of 1 mg/ml was adjusted. The SEC was equilibrated with PBS. 2 ml of lysate was injected to a HiPrep 16/60 Sephacryl S-400 column coupled to a liquid chromatography system (ÄKTAprime; GE Healthcare). Proteins were eluted with the equilibration buffer at a flow rate of 0.5 ml/min and detected spectrophotometrically at 280 nm. SEC fractions of 4.5 ml were collected and further analyzed for TDP-43 luciferase assay or dot blots. For the luciferase assay, 100-µl eluate of each fraction was pipetted into a white 96-well plate, and luciferase activity was measured as described in the Materials and methods paragraph Luciferase assay.

Biochemical fractionation

To examine the effect of sorbitol on the solubility profiles of wild-type TDP-43, sequential protein extractions were performed to separate into detergent-soluble and -insoluble fractions. Treated cells were washed twice with cold 1× PBS and lysed in 70 µl of cold radioimmunoprecipitation assay buffer (50-mM Tris-HCl, pH 8, 150-mM NaCl, 1% NP-40, 0.1% SDS, and 0.5-mM sodium deoxycholate) with 1× Halt protease inhibitor cocktail and 1× phosphatase inhibitor cocktail (PhosSTOP; Roche). Afterward, cells were sonicated for 30 min. After determination of the protein concentration by a BCA protein assay, lysates were adjusted to equal concentrations and volumes. After centrifugation for 30 min at 100,000 g and 4°C, the supernatants were collected as the soluble fractions. To prevent contamination caused by protein carryover, the pellets were resonicated twice and recentrifuged with 200 µl of fresh radioimmunoprecipitation assay buffer for 30 min at 100,000 g and 4°C. The pellets were dissolved in urea buffer (8-M urea, 10-mM Tris, and 50-mM NaH_2PO_4, pH 8.0). The total soluble and insoluble proteins were analyzed by Western blotting.

Immunocytochemistry

HEK-293 cells were grown in poly-D-lysine–coated (Sigma-Aldrich) coverslips. After treatment, the cells were rinsed with PBS twice, fixed for 10 min in 4% paraformaldehyde, and permeabilized for 10 min with 0.1% Triton X-100 and 100-mM glycine in PBS. The cells were blocked for 60 min with PBT (PBS + 1.5% BSA and 0.1% Tween 20). Primary antibodies used were rabbit anti–TDP-43 (1:500; 10782-2-AP; Proteintech Group, Inc.), mouse anti–TIA-1 related protein (TIAR; 1:500; BD), and mouse anti–α-smooth muscle actin (1:100; A2547; Sigma-Aldrich). Secondary antibodies used were goat anti–mouse IgG, DyLight 488, goat anti–rabbit IgG, DyLight 594 (both 1:750; Thermo Fisher Scientific), and donkey anti–mouse IgG Alexa Fluor 647 (1:750;

A31571; Life Technologies). Primary antibodies were diluted in PBT and incubated with the coverslip for 60 min. After washing the cells twice with PBS, they were incubated with the secondary antibody for 60 min in the dark. Cells were washed three times with PBS and mounted in mowiol containing DAPI.

Nuclear to cytoplasmic fractionation

48 h after transfection, the cells were treated with or without sorbitol. After 1 h, cells were rinsed twice with PBS and then harvested in fractionation buffer (10-mM Tris, pH 7.0, and 250-mM sucrose). After centrifugation at 750 *g* for 5 min, the supernatant was removed, and 1 ml of fresh fractionation buffer was added. Cells were lysed using a douncer, protein concentration was determined using a BCA assay, and total protein was adjusted to 1 mg/ml in each sample. The samples were centrifuged for 2 min at 2,000 *g* to remove unlysed cells. The supernatant was recentrifuged for 2 min at 4,000 *g*. The pellet contained the nuclear fraction, whereas the cytoplasmic fraction was in the supernatant. To avoid cross-contamination, the pellet was washed with fractionation buffer and recentrifuged. The fractions were analyzed using the luciferase assay.

Caspase assay

Primary cortical mouse neurons were grown in 96-well plates. At 7 DIV, MVEs and MVE-free supernatant were added to the neurons. After 72 h, the activity of caspase-3/7 was measured using the Apo-ONE homogeneous caspase-3/7 assay (Promega) according to the manufacturer's protocol.

Antibodies used for Western blots

Primary antibodies used at 1:1,000 in Tris-buffered saline + Tween 20 (TBST) were rabbit anti–TDP-43 antibody (10782-2-AP; Proteintech Group), rabbit anti–β-actin antibody (13E5; Cell Signaling Technology), mouse anti–myc-Tag antibody (9B11; Cell Signaling Technology), mouse anti–flotillin-1 antibody, mouse anti-GM130 antibody, mouse anti–Bcl-2 antibody (BD), and rabbit anti-CD63 antibody (h193; Santa Cruz Biotechnology, Inc.). Secondary antibodies (1:1,000) used were goat anti–rabbit or goat anti–mouse IgGs (Life Technologies).

Dot blot

Eluates of SEC fractions were collected as described in the Materials and methods paragraph SEC, and 350 µl of each fraction was applied to a nitrocellulose membrane (0.22-µm pore size; Protran; Whatman) placed in a dot blot apparatus (Schleicher & Schuell Minifold-I Dot-Blot System; Whatman). Samples were filtered through the membrane by vacuum and developed using conditions as described in the previous section.

TDP-43 coimmunoprecipitation

To prepare cell lysates for immunoprecipitation, 48 h after transfection, HEK-293 cells were washed with PBS and scraped in 300 µl lysis buffer (100-mM NaCl, 50-mM Tris-HCl, 5-mM EDTA, 0.3% [vol/vol] Triton X-100, and 5% complete mini-protease inhibitor, pH 7.4) and incubated on ice for 20 min. Lysates were centrifuged at 10,000 *g* for 10 min at 4°C. The protein concentration of the lysates was quantified by BCA protein assay kit, and the lysates were adjusted to equal protein concentrations. To remove unspecific protein binding to the beads, lysate were precleared by incubation with 20 µl Protein A mag Sepharose Xtra magnetic beads (GE Healthcare) for 1 h at 4°C with end-over rotation. Afterward, beads were separated from the lysates by means of a magnet, and the precleared lysates were then used for immunoprecipitation. To prepare magnetic beads for immunoprecipitation, magnetic beads were washed with lysis buffer and

incubated with lysis buffer with 0.6% (vol/vol) rabbit anti-*G. princeps* luciferase antibody (401P; Nanolight) and 2% BSA overnight at 4°C with end-over rotation. After that, beads were washed three times with lysis buffer. For immunoprecipitation, the prepared beads were incubated with the precleared lysates for 2 h at 4°C with end-over rotation, followed by three washing steps with lysis buffer. Beads were eluted by boiling them for 5 min at 95°C in 35 µl of 4× loading buffer (according to NuPAGE LDS sample buffer recipe + 80-mM DTT). The immunoprecipitation samples and the cell lysates (input) were separated by SDS-PAGE and transferred to polyvinylidene fluoride membrane. TDP-43 was detected with rabbit anti–TDP-43 antibody (1:1,000) and Clean blot IP detection reagent kit (Thermo Fisher Scientific) according to the manufacturer's instructions.

MVE purification

MVEs from HEK-293 cells and primary neurons were prepared as described previously (Thery et al., 2006). In brief, CM was collected 60 h after medium change, and the supernatant was centrifuged for 10 min at 500 *g*, 10 min at 2,000 *g*, and 30 min at 10,000 *g* with all steps at 4°C. Afterward, the supernatant was ultracentrifuged at 150,000 *g* for 90 min, and the MVE pellet was resuspended in PBS and recentrifuged at 150,000 *g* for 70 min to remove contaminating proteins. The final MVE pellet was resuspended in PBS for Western blotting or luciferase assay and in Opti-Mem for cell treatment, respectively.

Characterization of MVEs by nanoparticle tracking analysis

Analysis of absolute size distribution of CM before ultracentrifugation, MVEs, and the corresponding MVE-free supernatant after ultracentrifugation was performed using a NanoSight LM10 as instructed by the manufacturer. Three measurements for 90 s were performed for each sample.

EM sample preparation and immunogold labeling

High pressure freezing, freeze substitution, and embedding were performed as previously described (Wilkat et al., 2014) with minor changes. Freeze substitution was performed for London Resin gold embedding. Ultrathin sections (80 nm thick) were blocked with 1% BSA in PBS, pH 7.6, and incubated for 30 min with polyclonal rabbit anti–TDP-43 antibody (1:20; 10782-2-AP; Proteintech Group, Inc.). After thoroughly washing with PBS, the sections were incubated for 30 min with the secondary antibody (goat anti-rabbit coupled to 10-nm gold particles; Aurion). The sections were postfixed with glutaraldehyde and poststained with uranyl acetate. TEM was performed as described in the following paragraph.

TEM

Ultrathin sections were imaged as previously described (Wilkat et al., 2014). In brief, microscopy was performed using a transmission electron microscope (JEM-1400; Jeol GmbH) at an acceleration voltage of 120 kV. The images were recorded with a digital camera (Veleta; Olympus) and iTEM software (Olympus). No additional image processing apart from brightness/contrast correction was performed.

Fabrication of neuronal microfluidic devices

The reusable soft lithography master mold was fabricated using standard SU-8 multilayer photolithography. For the first layer containing the connecting microgrooves, SU-8 2002 was spun at 1,000 rpm on a clean silicon wafer for 35 s to form a uniform film of SU-8 ~3-µm thick. After prebaking at 95°C for 2 min, the SU-8 was exposed through a photomask (CAD/Art Services Inc.) using a

Novacure 2100 Spot Curing System (EXFO Inc.). The 3-µm layer was completed after a 2-min postbake at 95°C and development with SU-8 developer (Microchem) for ~1 min. In a similar manner, the 100-µm-thick second layer forming the cell culture chambers was patterned by first spinning SU-8 2050 at 1,650 rpm for 35 s. The wafer was then prebaked at 65°C for 5 min and 95°C for 20 min before manually aligning the photomask with respect to the features of the 3-µm layer and exposing. Finally, after postbaking at 65°C for 1 min and 95°C for 10 min, the mold was completed by developing for ~10 min with SU-8 developer. The wafer was placed in a clean Petri dish and was treated with Sylgard 184 (Dow Corning) to facilitate removal of polydimethylsiloxane (PDMS) from the master mold. PDMS was prepared using a 10:1 ratio of the prepolymer and catalyst and poured on the wafer. After desiccating, the Petri dish containing the wafer and PDMS was placed in a dry oven for 2 h at 60°C. Glass coverslips were placed in 6-well plates and coated with poly-D-lysine (Sigma-Aldrich) at 10 µg/ml in sterile H_2O at room temperature overnight. The coverslips were rinsed three times with water before being air dried. The PDMS devices were plasma cleaned and placed on the coverslips.

Uptake experiments

HEK-293 cells were transfected with mock, TDP-L1 + TDP-L2, or TDP-Luc, and a complete media change was performed after 12 h. CM was collected after an additional 60 h. Naive HEK-293 cells were cultured for 72 h in CM and washed three times with PBS, and luciferase activity was measured.

Primary cortical mouse neurons (5 DIV) were transduced with rAAV6.2 encoding TDP-L1 + TDP-L2 or TDP-Luc. Naive neurons were cultured in CM for 72 h and washed three times with PBS, and luciferase activity was measured.

Anterograde transport

Primary cortical mouse neurons (5 DIV) cultured in microfluidic devices were transduced with rAAV6.2 encoding TDP-Luc. At 24 h after transduction, a complete medium change was performed before H4 cells were plated in the axonal compartment. Excess culture medium was added to the axonal compartment during the entire experiment to maintain a positive hydraulic pressure and prevent diffusion of TDP-43 or virus particles. After 72 h, H4 cells were washed and harvested, and luciferase activity was measured.

Retrograde transport

CM from HEK-293 cells transfected with mock, Luc, or TDP-Luc was added to the axonal compartment of microfluidic devices containing primary cortical neurons (5 DIV). Excess culture medium was added to the cell body compartment to maintain a positive hydraulic pressure to avoid protein diffusion during the entire experiment. After 5 d, neuron bodies were harvested, washed, transferred to a 96-well plate, and analyzed for luciferase activity.

Seeding with CNS lysates

Native deeply frozen CNS tissue was solved in the ninefold volume of PBS (100 mg tissue + 900 µl PBS) and lysed using a TissueLyser (QIAGEN) twice for 2 min at 25 Hz. The lysate was centrifuged at 3,000 g for 10 min, the supernatant was transferred into a new tube, and the pellet was resolved in PBS and adjusted to an equal protein concentration of 2 µg/µl.

Primary cortical mouse neurons were grown in 96-well plates. At 5 DIV, the neurons were transduced by rAAV6.2 encoding TDP-L1 and TDP-L2. After 48 h, 5 µg CNS lysate was added to the neurons in triplicate. After an incubation of 4.5 h, the medium was replaced by PBS, and luciferase activity was measured immediately.

Microscopy

Microscopy of immunostained and fixed cells was performed at room temperature using a microscope (Axio Observer.A1; Carl Zeiss) equipped with LD Plan-NEOFLUAR 20×/0.4 and EC Plan-NEO FLUAR 63×/1.25 oil lenses (Carl Zeiss) and a digital camera (Axio-CamMRm; Carl Zeiss). The pictures were recorded using AxioVision Rel. 4.8 software (Carl Zeiss). Images were combined into figures for the manuscript using Photoshop (Adobe).

Confocal microscopy

Confocal images of immunostained and fixed cells were taken at room temperature using a laser-scanning microscope (LSM 710 NLO; Carl Zeiss) and an LD C-Apochromat 63×/1.15 W Korr objective. Z stacks and orthogonal micrographs were recorded using ZEN2010 software (Carl Zeiss). Images were combined into figures for the manuscript using Photoshop.

Statistical analysis

All results are presented as mean ± SEM and graphed using Prism5 (GraphPad Software). To identify the statistical significance, a two-tailed Student's t test using Prism (GraphPad Software) was performed.

Study approval and patient cohort

Appropriate approval and procedures were applied concerning human biomaterial. With informed written consent and approved by the national medical ethical review boards in accordance with the World Medical Association Declaration of Helsinki, CNS autopsies were obtained from individuals without neurological diseases and from patients with clinically and histopathologically confirmed ALS. Nonneurological controls were age and gender matched to the ALS patients (Table 1).

Online supplemental material

Fig. S1 shows size and purity assessment of HEK-293–derived MVEs. Fig. S2 demonstrates equal expression levels of the TDP-43 split VenusYFP constructs and proves the inactivity of the disrupted chromophore by microscopy analysis. Online supplemental material is available at http://www.jcb.org/cgi/content/full/jcb.201504057/DC1.

References

Braak, H., and E. Braak. 1991. Neuropathological stageing of Alzheimer-related changes. *Acta Neuropathol.* 82:239–259. http://dx.doi.org/10.1007/BF00308809

Braak, H., K. Del Tredici, U. Rüb, R.A. de Vos, E.N. Jansen Steur, and E. Braak. 2003. Staging of brain pathology related to sporadic Parkinson's disease. *Neurobiol. Aging.* 24:197–211. http://dx.doi.org/10.1016/S0197-4580(02)00065-9

Braak, H., J. Brettschneider, A.C. Ludolph, V.M. Lee, J.Q. Trojanowski, and K. Del Tredici. 2013. Amyotrophic lateral sclerosis--a model of corticofugal axonal spread. *Nat. Rev. Neurol.* 9:708–714. http://dx.doi.org/10.1038/nrneurol.2013.221

Brettschneider, J., K. Del Tredici, J.B. Toledo, J.L. Robinson, D.J. Irwin, M. Grossman, E. Suh, V.M. Van Deerlin, E.M. Wood, Y. Baek, et al.. 2013. Stages of pTDP-43 pathology in amyotrophic lateral sclerosis. *Ann. Neurol.* 74:20–38. http://dx.doi.org/10.1002/ana.23937

Brettschneider, J., K. Arai, K. Del Tredici, J.B. Toledo, J.L. Robinson, E.B. Lee, S. Kuwabara, K. Shibuya, D.J. Irwin, L. Fang, et al. 2014. TDP-43 pathology and neuronal loss in amyotrophic lateral sclerosis spinal cord. *Acta Neuropathol.* 128:423–437. http://dx.doi.org/10.1007/s00401-014-1299-6

Budini, M., E. Buratti, C. Stuani, C. Guarnaccia, V. Romano, L. De Conti, and F.E. Baralle. 2012. Cellular model of TAR DNA-binding protein 43 (TDP-43) aggregation based on its C-terminal Gln/Asn-rich region. *J. Biol. Chem.* 287:7512–7525. http://dx.doi.org/10.1074/jbc.M111.288720

Charcot, J.M. 1874. Amyotrophies spinales deuteropathiques sclérose latérale amyotrophique & sclérose latérale amyotrophique. *Bureaux du Progrès Médical.* 2:234–266.

Chernyshev, V.S., R. Rachamadugu, Y.H. Tseng, D.M. Belnap, Y. Jia, K.J. Branch, A.E. Butterfield, L.F. Pease III, P.S. Bernard, and M. Skliar. 2015. Size and shape characterization of hydrated and desiccated exosomes. *Anal. Bioanal. Chem.* 407:3285–3301. http://dx.doi.org/10.1007/s00216-015-8535-3

Danzer, K.M., S.K. Krebs, M. Wolff, G. Birk, and B. Hengerer. 2009. Seeding induced by α-synuclein oligomers provides evidence for spreading of α-synuclein pathology. *J. Neurochem.* 111:192–203. http://dx.doi.org/10.1111/j.1471-4159.2009.06324.x

Danzer, K.M., W.P. Ruf, P. Putcha, D. Joyner, T. Hashimoto, C. Glabe, B.T. Hyman, and P.J. McLean. 2011. Heat-shock protein 70 modulates toxic extracellular α-synuclein oligomers and rescues trans-synaptic toxicity. *FASEB J.* 25:326–336. http://dx.doi.org/10.1096/fj.10-164624

Danzer, K.M., L.R. Kranich, W.P. Ruf, O. Cagsal-Getkin, A.R. Winslow, L. Zhu, C.R. Vanderburg, and P.J. McLean. 2012. Exosomal cell-to-cell transmission of alpha synuclein oligomers. *Mol. Neurodegener.* 7:42. http://dx.doi.org/10.1186/1750-1326-7-42

Dewey, C.M., B. Cenik, C.F. Sephton, D.R. Dries, P. Mayer III, S.K. Good, B.A. Johnson, J. Herz, and G. Yu. 2011. TDP-43 is directed to stress granules by sorbitol, a novel physiological osmotic and oxidative stressor. *Mol. Cell. Biol.* 31:1098–1108. http://dx.doi.org/10.1128/MCB.01279-10

Feneberg, E., P. Steinacker, S. Lehnert, A. Schneider, P. Walther, D.R. Thal, M. Linsenmeier, A.C. Ludolph, and M. Otto. 2014. Limited role of free TDP-43 as a diagnostic tool in neurodegenerative diseases. *Amyotroph. Lateral Scler. Frontotemporal Degener.* 15:351–356. http://dx.doi.org/10.3109/21678421.2014.905606

Fiesel, F.C., and P.J. Kahle. 2011. TDP-43 and FUS/TLS: cellular functions and implications for neurodegeneration. *FEBS J.* 278:3550–3568. http://dx.doi.org/10.1111/j.1742-4658.2011.08258.x

Goedert, M., B. Falcon, F. Clavaguera, and M. Tolnay. 2014. Prion-like mechanisms in the pathogenesis of tauopathies and synucleinopathies. *Curr. Neurol. Neurosci. Rep.* 14:495. http://dx.doi.org/10.1007/s11910-014-0495-z

Gowers, W.R. 1886. A Manual of Diseases of the Nervous System. J & A Churchill, London. 992 pp.

Igaz, L.M., L.K. Kwong, E.B. Lee, A. Chen-Plotkin, E. Swanson, T. Unger, J. Malunda, Y. Xu, M.J. Winton, J.Q. Trojanowski, and V.M. Lee. 2011. Dysregulation of the ALS-associated gene TDP-43 leads to neuronal death and degeneration in mice. *J. Clin. Invest.* 121:726–738. http://dx.doi.org/10.1172/JCI44867

Johnson, B.S., D. Snead, J.J. Lee, J.M. McCaffery, J. Shorter, and A.D. Gitler. 2009. TDP-43 is intrinsically aggregation-prone, and amyotrophic lateral sclerosis-linked mutations accelerate aggregation and increase toxicity. *J. Biol. Chem.* 284:20329–20339. http://dx.doi.org/10.1074/jbc.M109.010264

Kanouchi, T., T. Ohkubo, and T. Yokota. 2012. Can regional spreading of amyotrophic lateral sclerosis motor symptoms be explained by prion-like propagation? *J. Neurol. Neurosurg. Psychiatry.* 83:739–745. http://dx.doi.org/10.1136/jnnp-2011-301826

Kawahara, Y., and A. Mieda-Sato. 2012. TDP-43 promotes microRNA biogenesis as a component of the Drosha and Dicer complexes. *Proc. Natl. Acad. Sci. USA.* 109:3347–3352. http://dx.doi.org/10.1073/pnas.1112427109

Luk, K.C., C. Song, P. O'Brien, A. Stieber, J.R. Branch, K.R. Brunden, J.Q. Trojanowski, and V.M. Lee. 2009. Exogenous α-synuclein fibrils seed the formation of Lewy body-like intracellular inclusions in cultured cells. *Proc. Natl. Acad. Sci. USA.* 106:20051–20056. http://dx.doi.org/10.1073/pnas.0908005106

Luk, K.C., V.M. Kehm, B. Zhang, P. O'Brien, J.Q. Trojanowski, and V.M. Lee. 2012. Intracerebral inoculation of pathological α-synuclein initiates a rapidly progressive neurodegenerative α-synucleinopathy in mice. *J. Exp. Med.* 209:975–986. http://dx.doi.org/10.1084/jem.20112457

Maniecka, Z., and M. Polymenidou. 2015. From nucleation to widespread propagation: A prion-like concept for ALS. *Virus Res.* 207:94–105. http://dx.doi.org/10.1016/j.virusres.2014.12.032

Masuda-Suzukake, M., T. Nonaka, M. Hosokawa, T. Oikawa, T. Arai, H. Akiyama, D.M. Mann, and M. Hasegawa. 2013. Prion-like spreading of pathological α-synuclein in brain. *Brain.* 136:1128–1138. http://dx.doi.org/10.1093/brain/awt037

Meyer-Luehmann, M., J. Coomaraswamy, T. Bolmont, S. Kaeser, C. Schaefer, E. Kilger, A. Neuenschwander, D. Abramowski, P. Frey, A.L. Jaton, et al. 2006. Exogenous induction of cerebral β-amyloidogenesis is governed by agent and host. *Science.* 313:1781–1784. http://dx.doi.org/10.1126/science.1131864

Neumann, M., D.M. Sampathu, L.K. Kwong, A.C. Truax, M.C. Micsenyi, T.T. Chou, J. Bruce, T. Schuck, M. Grossman, C.M. Clark, et al. 2006. Ubiquitinated TDP-43 in frontotemporal lobar degeneration and amyotrophic lateral sclerosis. *Science.* 314:130–133. http://dx.doi.org/10.1126/science.1134108

Neumann, M., L.K. Kwong, E.B. Lee, E. Kremmer, A. Flatley, Y. Xu, M.S. Forman, D. Troost, H.A. Kretzschmar, J.Q. Trojanowski, and V.M. Lee. 2009. Phosphorylation of S409/410 of TDP-43 is a consistent feature in all sporadic and familial forms of TDP-43 proteinopathies. *Acta Neuropathol.* 117:137–149. http://dx.doi.org/10.1007/s00401-008-0477-9

Nishihira, Y., C.F. Tan, Y. Hoshi, K. Iwanaga, M. Yamada, I. Kawachi, M. Tsujihata, I. Hozumi, T. Morita, O. Onodera, et al. 2009. Sporadic amyotrophic lateral sclerosis of long duration is associated with relatively mild TDP-43 pathology. *Acta Neuropathol.* 117:45–53. http://dx.doi.org/10.1007/s00401-008-0443-6

Nonaka, T., M. Masuda-Suzukake, T. Arai, Y. Hasegawa, H. Akatsu, T. Obi, M. Yoshida, S. Murayama, D.M. Mann, H. Akiyama, and M. Hasegawa. 2013. Prion-like properties of pathological TDP-43 aggregates from diseased brains. *Cell Reports.* 4:124–134. http://dx.doi.org/10.1016/j.celrep.2013.06.007

Outeiro, T.F., P. Putcha, J.E. Tetzlaff, R. Spoelgen, M. Koker, F. Carvalho, B.T. Hyman, and P.J. McLean 2008 Formation of toxic oligomeric a-synuclein species in living cells. PLoS One. 2:e1867. http://dx.doi.org/10.1371/journal.pone.0001867

Pasinelli, P., and R.H. Brown. 2006. Molecular biology of amyotrophic lateral sclerosis: insights from genetics. *Nat. Rev. Neurosci.* 7:710–723. http://dx.doi.org/10.1038/nrn1971

Pesiridis, G.S., V.M. Lee, and J.Q. Trojanowski. 2009. Mutations in TDP-43 link glycine-rich domain functions to amyotrophic lateral sclerosis. *Hum. Mol. Genet.* 18(R2):R156–R162. http://dx.doi.org/10.1093/hmg/ddp303

Polymenidou, M., and D.W. Cleveland. 2011. The seeds of neurodegeneration: prion-like spreading in ALS. *Cell.* 147:498–508. http://dx.doi.org/10.1016/j.cell.2011.10.011

Ravits, J.M., and A.R. La Spada. 2009. ALS motor phenotype heterogeneity, focality, and spread: deconstructing motor neuron degeneration. *Neurology.* 73:805–811. http://dx.doi.org/10.1212/WNL.0b013e3181b6bbbd

Remy, I., and S.W. Michnick. 2006. A highly sensitive protein-protein interaction assay based on *Gaussia* luciferase. *Nat. Methods.* 3:977–979. http://dx.doi.org/10.1038/nmeth979

Reyes, J.F., T.T. Olsson, J.T. Lamberts, M.J. Devine, T. Kunath, and P. Brundin. 2014. A cell culture model for monitoring α-synuclein cell-to-cell transfer. *Neurobiol. Dis.* 77:266–275. http://dx.doi.org/10.1016/j.nbd.2014.07.003

Sato, H., T. Kato, and S. Arawaka. 2014. Potential of cellular and animal models based on a prion-like propagation of α-synuclein for assessing antiparkinson agents. *Mol. Neurobiol.*

Sreedharan, J., I.P. Blair, V.B. Tripathi, X. Hu, C. Vance, B. Rogelj, S. Ackerley, J.C. Durnall, K.L. Williams, E. Buratti, et al. 2008. TDP-43 mutations in familial and sporadic amyotrophic lateral sclerosis. *Science.* 319:1668–1672. http://dx.doi.org/10.1126/science.1154584

Strobel, B., F.D. Miller, W. Rist, and T. Lamla. 2015. Comparative analysis of cesium chloride- and iodixanol-based purification of recombinant Adeno-associated virus (AAV) vectors for preclinical applications. *Hum. Gene Ther. Methods.* 26:147–157. http://dx.doi.org/10.1089/hgtb.2015.051

Tannous, B.A., D.E. Kim, J.L. Fernandez, R. Weissleder, and X.O. Breakefield. 2005. Codon-optimized *Gaussia* luciferase cDNA for mammalian gene expression in culture and *in vivo. Mol. Ther.* 11:435–443. http://dx.doi.org/10.1016/j.ymthe.2004.10.016

Thery, C., S. Amigorena, G. Raposo, and A. Clayton. 2006. Isolation and characterization of exosomes from cell culture supernatants and biological fluids. *In* Current Protocols in Cell Biology. John Wiley & Sons Inc., New York. 3.22.1–3.22.29. http://dx.doi.org/10.1002/0471143030.cb0322s30

Tsai, K.J., C.H. Yang, Y.H. Fang, K.H. Cho, W.L. Chien, W.T. Wang, T.W. Wu, C.P. Lin, W.M. Fu, and C.K. Shen. 2010. Elevated expression of TDP-43 in the forebrain of mice is sufficient to cause neurological and pathological phenotypes mimicking FTLD-U. *J. Exp. Med.* 207:1661–1673. http://dx.doi.org/10.1084/jem.20092164

Wilkat, M., E. Herdoiza, V. Forsbach-Birk, P. Walther, and A. Essig. 2014. Electron tomography and cryo-SEM characterization reveals novel ultrastructural features of host-parasite interaction during *Chlamydia abortus* infection. *Histochem. Cell Biol.* 142:171–184. http://dx.doi.org/10.1007/s00418-014-1189-y

Wils, H., G. Kleinberger, J. Janssens, S. Pereson, G. Joris, I. Cuijt, V. Smits, C. Ceuterick-de Groote, C. Van Broeckhoven, and S. Kumar-Singh. 2010. TDP-43 transgenic mice develop spastic paralysis and neuronal inclusions characteristic of ALS and frontotemporal lobar degeneration. *Proc. Natl. Acad. Sci. USA.* 107:3858–3863. http://dx.doi.org/10.1073/pnas.0912417107

Xu, Y.F., T.F. Gendron, Y.J. Zhang, W.L. Lin, S. D'Alton, H. Sheng, M.C. Casey, J. Tong, J. Knight, X. Yu, et al. 2010. Wild-type human TDP-43 expression causes TDP-43 phosphorylation, mitochondrial aggregation, motor deficits, and early mortality in transgenic mice. *J. Neurosci.* 30:10851–10859. http://dx.doi.org/10.1523/JNEUROSCI.1630-10.2010

Zhang, Y.J., Y.F. Xu, C. Cook, T.F. Gendron, P. Roettges, C.D. Link, W.L. Lin, J. Tong, M. Castanedes-Casey, P. Ash, et al. 2009. Aberrant cleavage of TDP-43 enhances aggregation and cellular toxicity. *Proc. Natl. Acad. Sci. USA.* 106:7607–7612. http://dx.doi.org/10.1073/pnas.0900688106

Zhou, J., E.D. Gennatas, J.H. Kramer, B.L. Miller, and W.W. Seeley. 2012. Predicting regional neurodegeneration from the healthy brain functional connectome. *Neuron.* 73:1216–1227. http://dx.doi.org/10.1016/j.neuron.2012.03.004

Zhu, L., M. Xu, M. Yang, Y. Yang, Y. Li, J. Deng, L. Ruan, J. Liu, S. Du, X. Liu, et al. 2014. An ALS-mutant TDP-43 neurotoxic peptide adopts an anti-parallel β-structure and induces TDP-43 redistribution. *Hum. Mol. Genet.* 23:6863–6877. http://dx.doi.org/10.1093/hmg/ddu409